A Physical Model for the Kink Effect in InAlAs/InGaAs HEMT's

Mark H. Somerville, Alexander Ernst, and Jesús A. del Alamo, *Senior Member, IEEE*

***Abstract*—We present a new model for the the kink effect in InAlAs/InGaAs HEMT's. The model suggests that the kink is due to a threshold voltage shift which arises from a hole pile-up in the extrinsic source and an ensuing charging of the surface and/or the buffer-substrate interface. The model captures the many of the observed behaviors of the kink, including the kink's dependence on bias, time, temperature, illumination, and device structure. Using the model, we have developed a simple equivalent circuit, which reproduced well the kink's dc characteristics, its time evolution in the nanosecond range, and its dependence on illumination.**

***Index Terms*—HEMT, InAlAs, InGaAs, kink effect.**

I. Introduction

THERE is continuing interest in the origin and consequences of the kink effect in InAlAs/InGaAs HEMTs [1]–[5]. The kink is associated with reduced gain and excess noise at high frequencies, and may be related to on-state breakdown and premature burnout [6].

Conventional wisdom suggests that traps are responsible for the kink in InAlAs/InGaAs devices. In these models, high fields at the drain end of the device change the charge state of traps in the buffer or in the insulator [7]. This leads to a shift in threshold voltage, hence a rise in drain current. Several reports appear to support such a theory: kink suppression through the careful control of growth suggests that traps may be responsible [7], [8]. Recent work has argued that the frequency dependence, transient response, and illumination dependence of the kink are consistent with a trap hypothesis as well [1], [9].

However, there is a substantial body of evidence indicating that impact ionization is in some way associated with the kink. It has been reported that the kink is suppressed as the bandgap of the channel is increased [10]–[12]. It has also been shown that devices biased in the kink region show significant light emission [12], another clear signature of impact ionization in the channel. The well-known relationship between impact ionization and the kink in silicon-on-insulator (SOI) MOSFET's [13] motivated one group successfully to use a source-contacted p-layer beneath the channel for kink suppression in InAlAs/InGaAs HEMT's [14]; this result seems to imply that impact-ionization generated holes play a significant role in the kink. Additionally, simulations show that the kink disappears if the impact ionization mechanism is turned off in the simulator [3], [4], [15]. Finally, we have reported sidegate measurements establishing a direct relationship between impact ionization and the kink [16], [17], as well as transient measurements showing that the time constants associated with the kink are strongly correlated with the impact ionization rate [18].

These results have led to a number of kink models that invoke impact ionization, including hole trap charging beneath the gate in the insulator and in the buffer [19]; pure impact ionization [20], [21], source resistance reduction [3], [4], [22]; and SOI-type floating body effects [23], [24]. While each of these models give some insight into the kink, none adequately explain all of the kink's behavior. In particular, any model for the kink must explain:

- kink's peculiar bias dependence; [16];
- kink's dependence on illumination [1], [2];
- relationship between impact ionization and the kink [17];
- kink's dynamic behavior (particularly the bias-dependence of the time constants associated with the kink) [18];
- relationships between the kink and the recess (for example, why is the kink strengthened as the width of the source-side recess is increased?) [22], [25];
- kink's dependence on aging and surface treatments [5], [26].

We have recently carried out a several studies of the kink, including dc characterization [16], sidegate measurements [17], and large-signal transient measurements with nanosecond resolution [18]. In this work, we have combined the results of these measurements, as well as new measurements of the kink's temperature and illumination dependence, to develop a comprehensive picture of the kink. We show that all our experimental results can be explained by an impact-ionization based model where hole pile-up at the source shifts the threshold voltage of the device. This has allowed us to develop the first dynamic physical model and a complete equivalent circuit for the kink in InAlAs/InGaAs HEMT's.

II. Physical Model for the Kink

Several attempts to explain the kink based on some sort of hole accumulation in the source have been made. We have previously suggested a model in which holes accumulate in the channel beneath the recessed region of the source [16]. Suemitsu *et al.* have postulated a similar mechanism based on suppression of the source resistance due hole accumulation in the source [3], [4]. Although Suemitsu's work provides physical insight into the

Manuscript received August 31, 1999; revised January 4, 2000. This work was supported in part by Raytheon Company, the Joint Services Electronics Program under Contract DAAH04-95-1-0038, a JSEP Fellowship, and a Presidential Young Investigator Award from the National Science Foundation (915 7305-ECS). The review of this paper was arranged by Editor K. M. Lau.

M. H. Somerville is with the Deptartment of Physics and Astronomy, Vassar College, Poughkeepsie, NY 12604 USA (e-mail: masomerville@vassar.edu).

A. Alexander is with McKinsey and Company, Mexico City, Mexico.

J. A. del Alamo is with the Department of Electrical Enginering and Computer Science, Massachusetts Institute of Technology, Cambridge, MA 02139 USA.

Publisher Item Identifier S 0018-9383(00)03399-2.

origins of the kink, the expressions he derives are complicated and depend on precise knowledge of fields and hole concentrations throughout the device. More importantly, we believe that R_S reduction is not sufficient to explain the kink effect, especially in high performance devices and close to threshold, where there is little voltage drop on the extrinsic source. Some other effect must be present.

The starting point for our model is the idea that although source resistance reduction models seem problematic, it seems likely that hole accumulation in the source is somehow responsible for the kink. This assumption is based on significant experimental evidence suggesting the importance of both holes and the extrinsic source in the kink effect. Recent reports of light emission from the extrinsic source [27] show clearly that a large number of impact-ionization generated holes in a normally-operating HEMT actually accumulate in the extrinsic source. Kink suppression by means of a buried source-contacted p-layer [24], [14] further motivate us to explore further the possible significance of holes and the source in the kink effect, as do experimental results showing the impact of the surface on the kink [26]. Can an accumulation of holes in the extrinsic source have some effect *other than* reducing R_S?

Careful consideration of the electrostatics and band configuration suggest a possible explanation for the kink. To simplify the problem, we present in Fig. 1 an idealized device cross-section. For simplicity, we assume that there is no cap or recess present. We further assume Fermi level pinning at the surface and at the buffer-substrate interface, and infinite recombination velocity at the ohmics. Because the vertical dimensions of the problem are much smaller than the horizontal dimensions, we initially impose the condition of quasineutrality in the vertical dimension—in other words, we require that the charge in any vertical "slice" of the device add to zero. At time $t = 0$, we assume that the device is biased at some value of $V_{\rm GS}$ above threshold, and at some reasonably high value of $V_{\rm DS}$ (above the value at which the kink would appear). Now, we examine how the kink evolves as a function of time if impact ionization is instantaneously "turned on" for $t > 0$ (see Fig. 1).

At $t = 0$ (no impact ionization), consider the conduction band along the vertical cut *A* on the source side of the gate. Vertical quasineutrality is satisfied by the requirement that the ionized dopant charge, the surface charge, and the charge at the substrate-buffer interface add to image the electrons in the channel. When impact ionization begins $(t > 0)$, holes are generated on the high-field drain end of the gate. These holes flow back through the channel toward the source, where they accumulate in the channel and recombine [16], [3]. A steady-state hole distribution *in the channel* is achieved in a time on the order of the hole transit time through the channel plus the recombination time τ in InGaAs—around 1 nS. Vertical quasineutrality is achieved through a minor increase in the electron concentration, as we expect the number of holes in the channel to be small relative to the number of electrons.

Although the holes at $t \approx \tau$ are in steady state within the channel, they are not in steady state vertically. Indeed, the hole quasi-Fermi level must bend in order to maintain Fermi pinning at the surface and the buffer. This will result in a small hole current to the surface and buffer [3], [4]. Let us assume that this

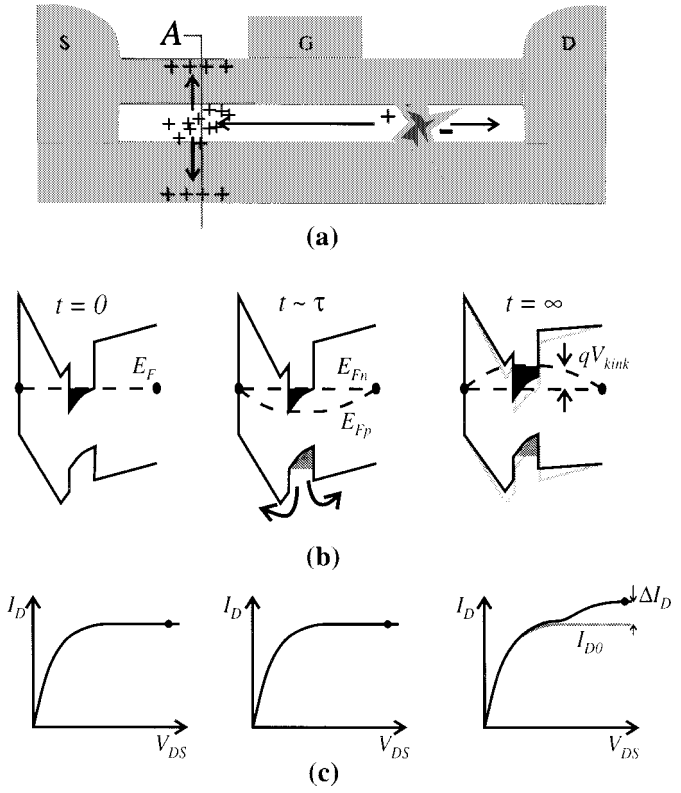

Fig. 1. Postulated kink mechanism. (a) Simplified device cross-section used for the model. (b) Energy bands within the extrinsic source adjacent to the gate as a function of time. (c) Drain current characteristics as a function of time.

hole current continues until the hole quasi-Fermi level is nearly flat. This is a fair approximation, given that the holes should be in better communication with the surface than the electrons (as evidenced by the dominance of hole current in I_G when the device is biased above the kink [17]). Note that the time for the holes to equilibrate with the surface and substrate-buffer interface will be significantly longer than the time to reach steady state in the channel, since they have to overcome a sizable energy barrier.

Of course, as holes reach the surface and the buffer-substrate interface, the charge at these locations changes. Vertical quasineutrality requires that this charge be imaged by additional electrons in the channel. This requirement raises the electron quasi-Fermi level and the potential of the channel. Suemitsu has suggested that since the Fermi level is pinned at the surface, the potential of the channel relative to the surface must approximately change by [3], [4]

$$V_{\rm kink} = \frac{k_B T}{q} \ln\left(\frac{p_0 + p'}{p_0}\right). \tag{1}$$

Here p_0 is the "pre-kink" hole concentration in the extrisic channel, and p' is the excess hole concentration there. A similar argument holds with respect to the buffer. Note that this expression suggests that the hole quasi-Fermi level is flat at steady state, and that the electron concentration has not changed by more than 10–20%. These are both reasonable assumptions. Note that although the electron gas is degenerate, a Boltzmann-type relationship remains appropriate for the holes.

In a real device, of course, the channel potential will change only by a fraction of $V_{\rm kink}$. This is because surface pinning should only be significant in the uncapped recess region; two dimensional effects thus imply that the size of $V_{\rm kink}$ will decrease as the length of the recess on the source side is reduced. Such an effect has been observed in simulations [4]. However, (1) does capture the key dependencies of the channel potential—it should depend logarithmically on the number of holes inside the channel in the extrinsic source.

Clearly this increase in channel potential, and ensuing change in electron concentration will result in an R_S reduction, as Suemitsu has argued [3], [4]. However, we believe the more important effect is the change in the channel potential *beneath the source end of the gate*. The vertical quasineutrality approximation made above ignores this effect, but of course, any change in electron concentration and channel potential in the region beside the gate necessarily implies a change in electron concentration and channel potential beneath the gate. This, in effect, changes the *threshold voltage* of the device. Thus, the transistor will experience additional drive through:

$$\Delta I_D \approx g_{m0} V_{\rm kink} \tag{2}$$

where ΔI_D is the "kink current", that is, the increase in I_D over its "pre-kink" value, I_{D0}. Again, two-dimensional (2-D) effects imply that this effect will be weaker than (1) suggests, but the functional dependence should not be modified.

Note that since impact ionization is occurring, the drain current should also rise due to the generated electrons and holes. However, we have previously established that the impact ionization current is low relative to the magnitude of the kink current [17]; we therefore neglect the ΔI_D contribution from pure impact ionization. For the same reason, we also do not include any linear threshold shift due to holes within the intrinsic device [28].

Before proceeding, it is worth noting that this model is *qualitatively* consistent with the kink's strange structural dependencies. If indeed charging of surface states or interface states is responsible for the kink, it is clear that changes in growth [7] or surface treatments [26] might suppress the kink by relaxing Fermi level pinning [3], [4]. Similarly, the two-dimensional effects discussed above help us to understand why the kink increases with the width of the recess—pinning will only occur in the region where the InGaAs cap is removed; the longer this region is, the closer the device comes to the simplified model presented above.

III. Equivalent Circuit Model

Using the picture presented above, we have formulated a simple, physically-based equivalent circuit that uses three bias-independent parameters to model both the transient and DC behavior of the kink, shown in Fig. 2. The model includes a current source, which represents the hole pileup provided by impact ionization. The current source feeds a parallel diode and capacitor, which represent the charging of the surface and/or buffer-substrate interface states by the hole current. Finally, a dependent voltage source in series with the source is controlled by the voltage across the capacitor; this voltage represents the change in channel potential, and thus the additional drive provided by the hole pile-up.

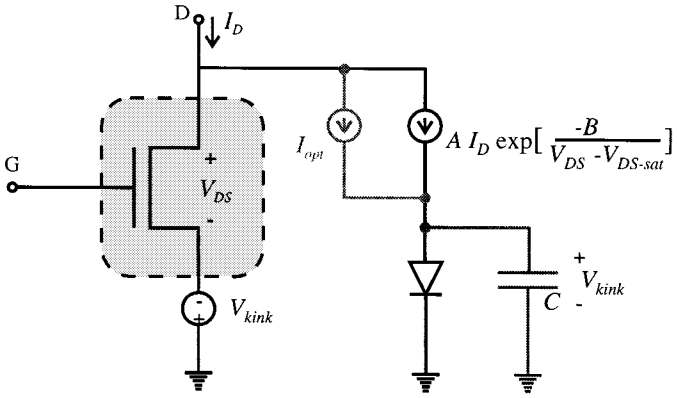

Fig. 2. Proposed large-signal transient kink equivalent circuit model. The model consists of an impact ionization current source, a channel diode with unity saturation current, and a capacitance. Three fitting parameters are needed: A and B in the impact ionization current source, and C, which relates to the capacitance of the channel with respect to the surface and the substrate. Also included (in gray) is a bias-independent photogeneration current, $I_{\rm opt}$, which describes the illumination dependence of the kink, as discussed in the text.

The bias dependence of the current source is determined according to the classical description of impact ionization. At a given temperature the ionization rate is proportional to the exponential of the inverse of the field in the high field region, as we have verified with the sidegate measurement [17], [30]. Furthermore, we expect that the number of excess holes in the extrinsic source to be directly proportional to the amount of impact ionization. Thus, the current source representing the holes is given by

$$I_{\rm impact} = AI_D \exp\left(\frac{-B}{V_{\rm DS} - V_{\rm DS\text{-}sat}}\right) \tag{3}$$

where A and B are temperature-dependent constants.

To minimize the number of fitting parameters, the diode is given a saturation current of unity ($I_0 = 1$ mA/mm). The final parameter is the normalized channel-surface/channel-substrate capacitance, C. It is worthwhile noting that *the absolute magnitudes of A and C have* **no** *physical meaning*, since they are only measured with respect to the arbitrary choice of 1 mA/mm for the diode saturation current.

Note that this equivalent circuit ignores the 2-D issues mentioned above. To include such effects, one could make the dependent voltage source proportional to, rather than equal to, the voltage across the capacitor. However, we have found that the addition of another fitting parameter to account for such effects is not necessary, as adjustment of A provides sufficient flexibility to account for such effects.

It must be emphasized that the form of this model is almost identical to that of SOI models [29]. This should not be surprising, given that in both cases the kink results from similar physics—impact ionization, hole accumulation, and a Boltzmann-type relationship relating potential to hole accumulation. It is important to note, though, that the detailed physical origins of the kink in the two models are significantly different—in partially-depleted SOI, the kink arises from forward biasing the source-body junction [29], whereas in this model, the kink is a

result of hole accumulation in the extrinsic source and the ensuing modification of the channel potential and electron concentration beneath the source end of the gate. While this difference has no impact on the form of the model, it is an important consideration when one attempts to engineer away the kink—if the kink is due to a floating body effect, one might try to suppress it by introducing an additional barrier in the valence band beneath the channel, or by increasing the resistivity of the buffer. On the other hand, if hole pile-up in the extrinsic source causes the kink, approaches such as passivating the surface in the source gate region (thereby relaxing Fermi level pinning) or introducing a hole barrier in the insulator might be more appropriate.

IV. Results

In order to test our model we have used lattice-matched, MBE-grown, HEMT's fabricated at MIT as a vehicle for this study [16], [18]. We examine devices with relatively long gate lengths ($L_G = 0.6$ μm to $L_G = 2$ μm). Due to the high aspect ratio of these devices, no significant short channel effects are observed, and the kink is expected to be relatively uncontaminated by such nonidealities. Indeed, no substantial change in the qualitative behavior of the kink is observed between $L_G = 0.6$ μm and $L_G = 2.0$ μm. As we discuss later, we believe our conclusions hold for shorter gate length devices as well, although performing the analysis in the presence of short channel effects is substantially more challenging.

For comparison of the model with our experiments, we have extracted the pre-kink current, I_{D0} and kink current, ΔI_D, as follows. For a given value of $V_{\rm GS}$, I_{D0} is defined as I_D at the point of minimum output conductance. Once I_{D0} is determined, ΔI_D is simply given by

$$\Delta I_D(V_{\rm DS}, V_{\rm GS}) = I_D(V_{\rm DS}, V_{\rm GS}) - I_{D0}(V_{\rm GS}). \quad (4)$$

Note that this definition *assumes* that the output conductance in the saturation regime is purely kink-related; in shorter devices, one would have to include a short-channel term as well.

A. DC Behavior

Before considering the detailed results of the equivalent circuit, we undertake a simple first-order analysis of our model, to demonstrate the consistency of the model with previously observed kink behaviors. We note first that at dc, from (1)–(3), the kink current can be described by the function

$$\Delta I_D \approx g_{m0}\frac{k_BT}{q}\ln\left[1 + AI_D\exp\left(\frac{-B}{V_{\rm DS} - V_{\rm DS\text{-}sat}}\right)\right]. \quad (5)$$

Thus, when the hole accumulation is large with respect to the pre-kink hole concentration, the exponential term dominates, so that at large $V_{\rm DS}$ values,

$$\Delta I_D|_{\text{large } V_{\rm DS}} \propto \frac{-1}{V_{\rm DS} - V_{\rm DS\text{-}sat}}. \quad (6)$$

To examine this behavior, we plot in Fig. 3 the magnitude of the kink versus $1/(V_{\rm DS} - V_{\rm DS\text{-}sat})$. Here we have measured the kink at low temperature, since the more pronounced low temperature kink facilitates more accurate extraction. As can be seen, the kink exhibits the expected linear dependence on

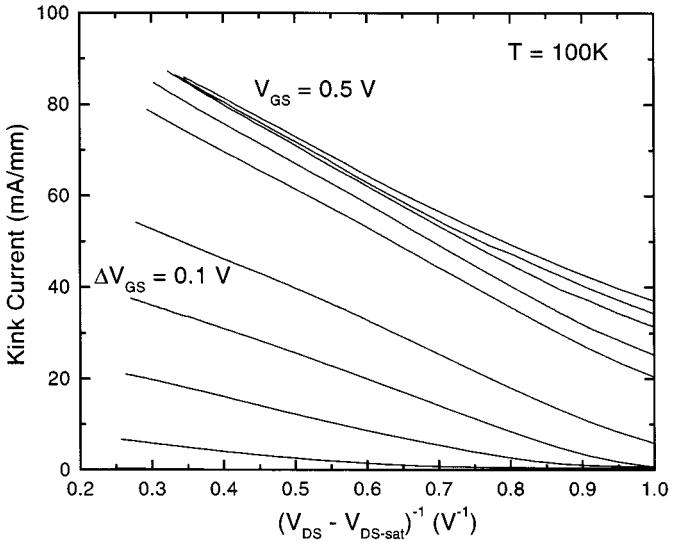

Fig. 3. Low temperature ($T = 100$ K) kink magnitude versus $1/(V_{\rm DS} - V_{\rm DS\text{-}sat})$. Note the linear behavior for all $V_{\rm GS}$ values. $L_G = 0.8$ μm.

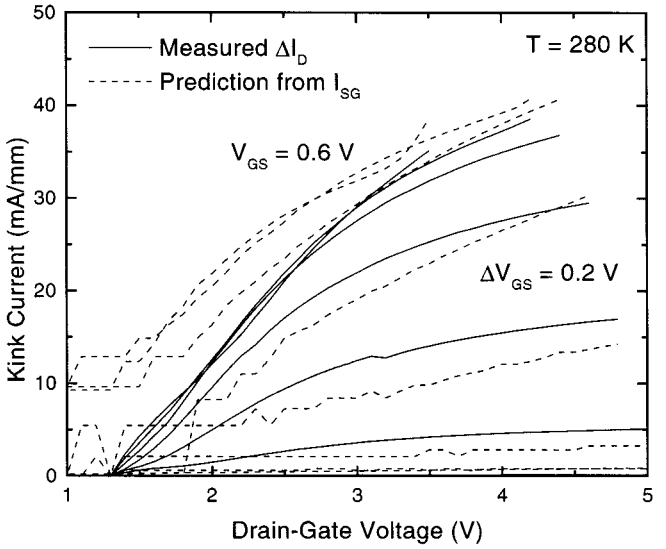

Fig. 4. Comparison of the kink current, ΔI_D, with the kink predicted by the sidegate current. $L_G = 2$ μm, $T = 280$ K.

$1/(V_{\rm DS} - V_{\rm DS\text{-}sat})$ for all $V_{\rm GS}$ values. Indeed, as we show in the following sections, (5) does a good job of describing the dc behavior of the kink in terms of output characteristics and output conductance for a wide variety of bias conditions.

The direct relationship between the sidegate current and impact ionization generation rate [30] implies that the kink should be predicted by the sidegate current. In particular,

$$\Delta I_D \approx g_{m0}\frac{k_BT}{q}\ln(1 + DI_{\rm SG}) \quad (7)$$

with D a bias-independent constant that scales the sidegate current. In order to test this, we have simultaneously measured the kink and the sidegate current. Fig. 4 compares the kink predicted by the sidegate current in this model with the measured kink current; as can be seen, the agreement is excellent. Note that only a single, bias-independent value of D is used for the entire data set.

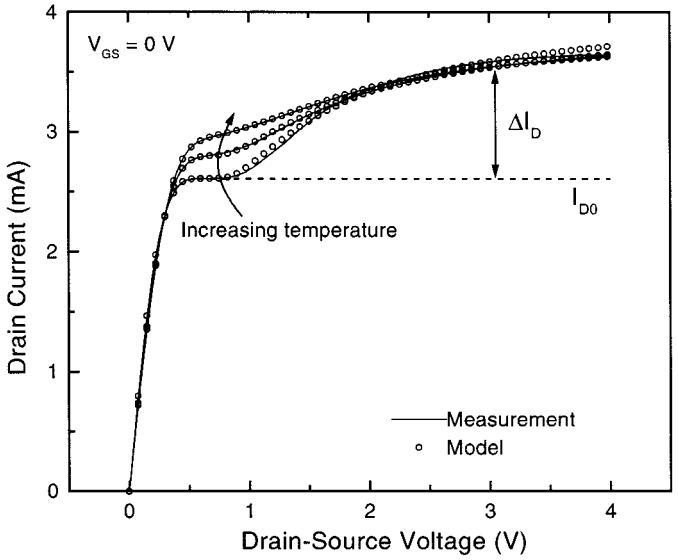

Fig. 5. Temperature dependence of the kink. Data is shown for 100 K, 280 K, and 350 K. The "pre-kink" drain current, I_{D0}, and kink magnitude, ΔI_D, are shown for the low-temperature data. Note that since the threshold voltage varies with temperature, it is not appropriate to compare the current magnitudes at different temperatures—one should compare ΔI_D instead. Also shown are results of the dc model, using different values of A and B at different temperatures.

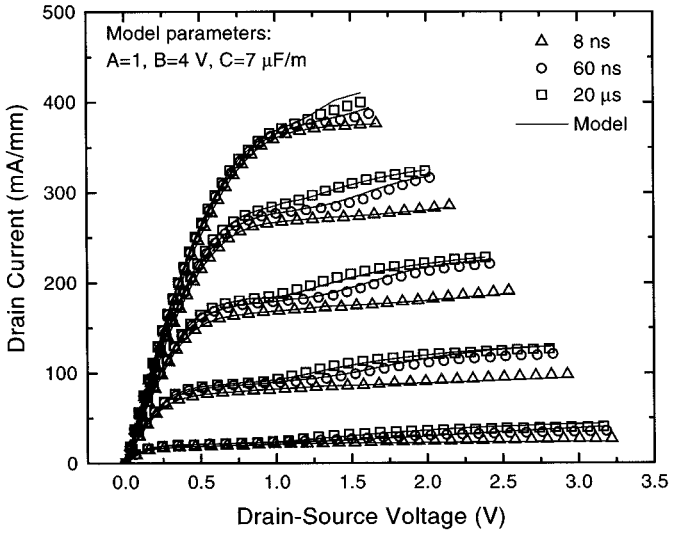

Fig. 6. Pulsed *I–V* curves measured at three different times. No kink is seen when the device is first turned on. The kink current, ΔI_D, turns on fastest at high values of $V_{\rm DS}$. Also shown are results from the equivalent circuit model shown in Fig. 1. Only three bias-independent constants are required to fit the kink for all the times considered.

B. Temperature Dependence

Before considering the detailed dynamic behavior of the kink, we briefly examine the kink's behavior as a function of temperature, summarized in Fig. 5. Devices were measured between 100 K and 350 K. As has been previously observed [9], [31], the kink becomes more sharply defined at low temperatures, and almost disappears at high temperatures, but the qualitative shape and the bias dependence of the kink do not change with temperature (in this figure, the change in the pre-kink current for low $V_{\rm DS}$ is due to a shift in V_T with temperature). This leads us to believe that the underlying physics of the kink is the same at low temperature as at high temperature.

Supporting this conclusion is the fact that at the equivalent circuit model describes the dc behavior well over a wide range of temperatures through appropriate choices of A and B. In general, modeling the kink at lower temperatures calls for using higher values of A, due to the strong temperature dependence of the background hole concentration, p_0, as well as the temperature dependence of impact ionization in InGaAs [32].

C. Transient Behavior

The transient behavior of the kink is also consistent with our model. Fig. 6 plots the measured and predicted large signal transient behavior of the kink. These measurements were performed using a carefully designed pulsed current–voltage (*I-V*) setup on an MBE-grown InAlAs/InGaAs single heterostructure HEMT with $L_G = 1.2\ \mu$m [18]. The measurement consists of pulsing the device from the off-state to the on-state along a 50 Ω load line, and measuring the resulting terminal voltages and currents as a function of time. The figure shows the resulting output characteristics at three times (8 nsec, 60 ns, and 20 μs). As can be seen, on short time scales the kink is almost nonexistent; it then builds first at higher drain voltages, and finally at lower drain voltages. This behavior is consistent with reports that the kink does not appear in high-frequency small signal measurements of output conductance [31]. As can be seen, the output characteristics predicted by the model agree closely with those measured throughout the measured domain, capturing both the initial rise of the kink at high $V_{\rm DS}$, and its subsequent saturation. Particularly important to note is the fact that even relatively close to threshold, ($I_D < 50$ mA/mm), the kink is significant. Such an effect is predicted by the equivalent circuit model.

To more rigorously test the model, we plot in Fig. 7 the kink output conductance, defined as the derivative of the predicted kink current with respect to the drain-source voltage, together with the actual output conductance for this device, measured at these three different times. Note that no other source of output conductance has been introduced in the model. As can be seen, the measured output conductance exhibits a strong time-dependent dispersion; similar effects have previously been attributed to traps [9]. The hole pile-up model accurately follows this dispersion in g_d, without appealing to any particular trap characteristics (other than Fermi level pinning). Indeed, the model predicts g_d throughout the saturation region.

A final test of the model's dynamic behavior is to examine the kink as a function of time (Fig. 8). Here we have plotted the extracted kink current (following the extraction method above) and the modeled kink current for different combinations of $V_{\rm DS}$ and $V_{\rm GS}$. As can be seen, the model works very well, predicting the shape, magnitude, and timing of the transient kink both at larger drain voltages, where the kink is a relatively fast phenomenon, and at smaller drain voltages, where the kink rises much more slowly. Indeed, the model now explains the previously observed dependence of kink rise time on impact ionization rate [18]. We believe that the slow transient in the μs range may be due to self-heating.

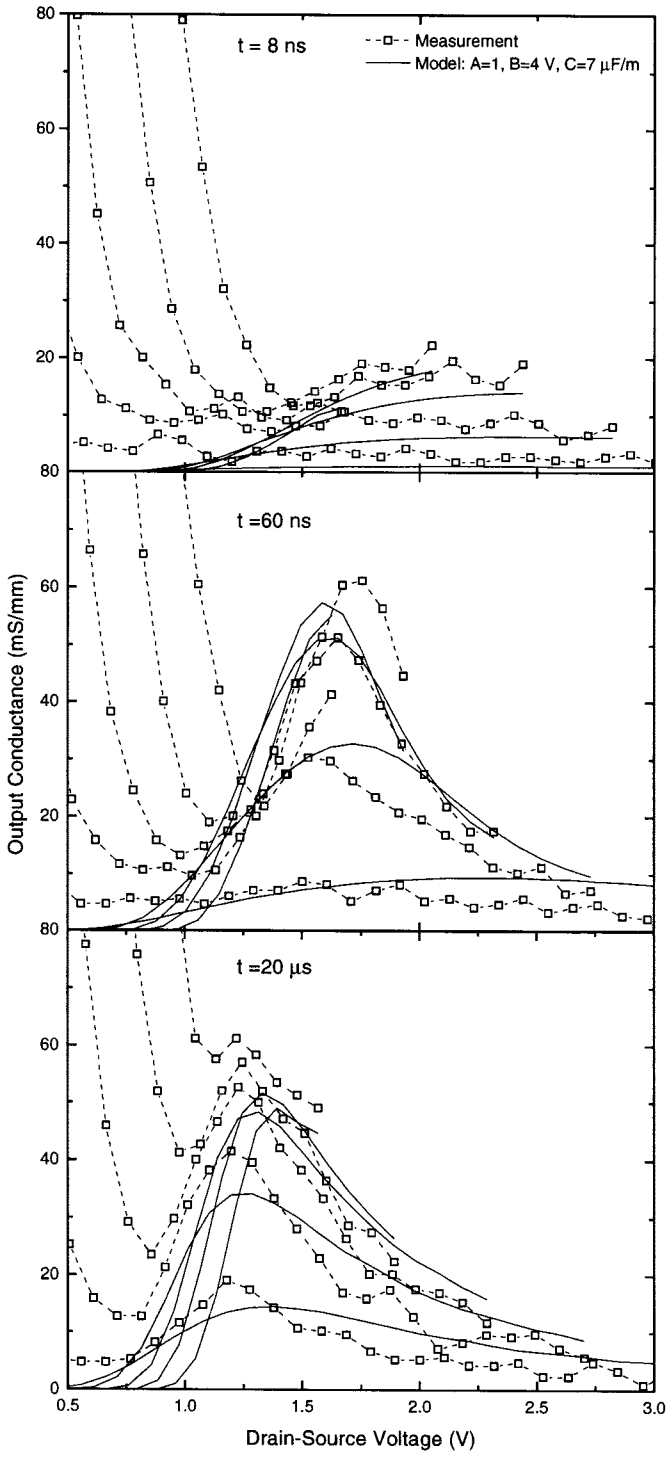

Fig. 7. Measured and modeled output conductance for $t = 8$ ns, $t = 60$ ns, and $t = 20\mu$ s. Different lines correspond to different values of $V_{\rm GS}$. $T =$ K.

D. Illumination

Recent work on the kink has focused in part on its illumination dependence [19], [1], [2]. The kink is known to be suppressed when the device is illuminated, as shown in Fig. 9. Here we have measured one of our device's output characteristics and transfer characteristics under different levels of illumination with white light at $T =$220 K, where the kink is better defined. As can be seen, under illumination the kink weakens. Further

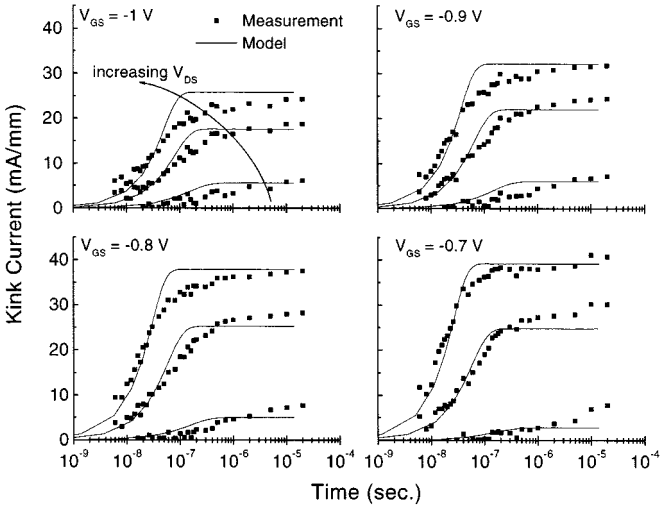

Fig. 8. Kink current as a function of time for different bias conditions, with predictions of the model. At each value of $V_{\rm GS}$, data is displayed for $V_{\rm DS} =$ 1.1 V, 1.6 V, and 2.1 V. As in Figs. 6 and 7, $A = 1, B = 4$ V, and $C = 7\ \mu$F/m. $T =$300 K.

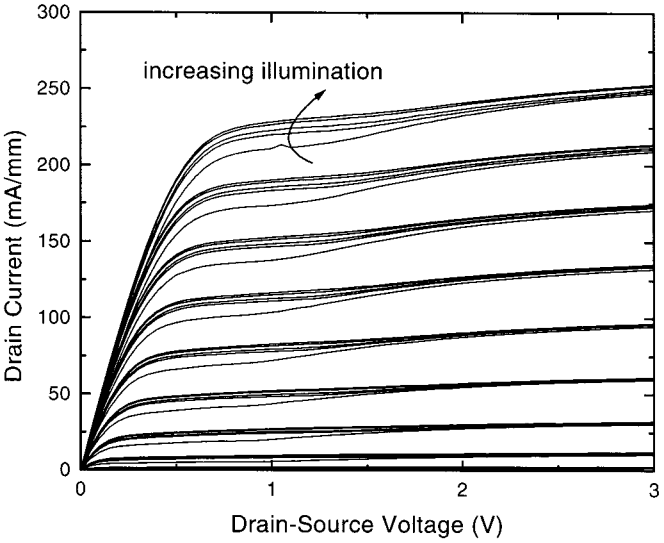

Fig. 9. Output characteristics measured with different levels of illumination ($T = 220$ K). The kink disappears as light intensity is increased.

more,the pre-kink current rises under illumination, while the post-kink current changes very little. This effect has been attributed both to photon-induced emptying of trap levels [1], as well as changes in the pre-kink hole concentration due to photo-generation [19], [2].

Our model predicts that such optically-generated holes will have *exactly the same effect as holes generated by impact ionization*—they will accumulate in the extrinsic source, and gradually modify the potential of the channel, yielding a threshold voltage shift as well as a small decrease in the source resistance as suggested by Suemitsu [3], [4]. In order to examine this, we plot in Fig. 10 the pre-kink ($V_{\rm DS} = 0.5$ V) transconductance as a function of illumination intensity. As can be seen, there is indeed a shift in the pre-kink threshold voltage, as well as a possible drop in r_s.

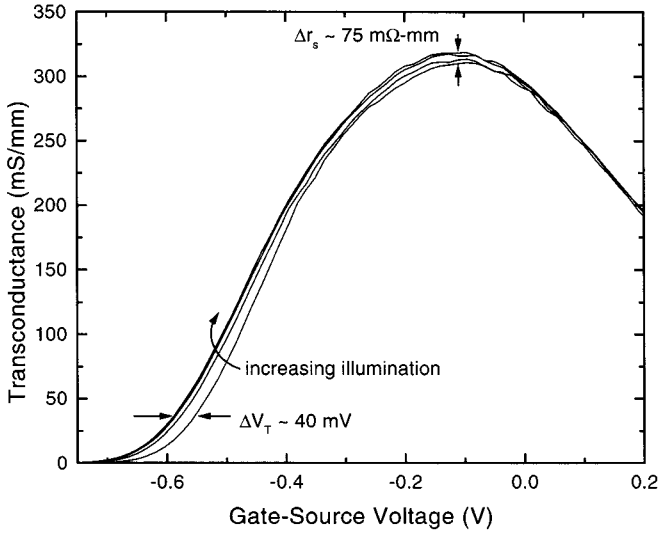

Fig. 10. Pre-kink ($V_{\rm DS} = 0.5$ V) transfer characteristics with and without illumination. Under illumination, the device exhibits a threshold voltage shift and reduction in source resistance consistent with increased hole concentration in the extrinsic source. $T = 220$ K.

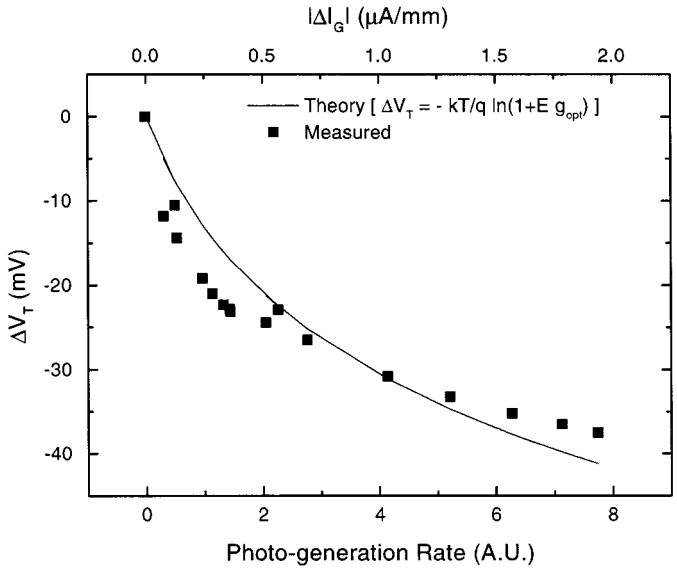

Fig. 11. Shift in pre-kink V_T as a function of optical generation rate, as determined by reverse gate current. The device exhibits a V_T shift that is logarithmic in the number of optically generated holes. $T = 220$ K.

According to the model, the V_T shift should be logarithmic in the number of excess holes. Thus, under illumination, we expect

$$\Delta V_T = -V_{\rm kink} = -\frac{k_B T}{q} \ln(1 + E g_{\rm opt}) \tag{8}$$

where $g_{\rm opt}$ is the optical generation rate and E is a constant relating the generation rate to the hole concentration in the extrinsic source.

To clarify this dependence, we have determined the relative optical generation rate in the device by measuring the difference between the reverse gate current at $V_{\rm GS} = -0.8$ V under illumination and the dark reverse gate current under the same bias condition. This measurement was performed at the same time as the transfer characteristics; the change in gate current is assumed to be directly proportional to the change in the generation rate. Fig. 11 uses the results of these measurements to plot the change in the threshold voltage as a function of the optical generation rate. As can be seen, the shift in V_T is well-described by (8). Recently Takanashi et al. have reported similar results by measuring the threshold voltage shift as a function of optical power using a monochromatic light source [2].

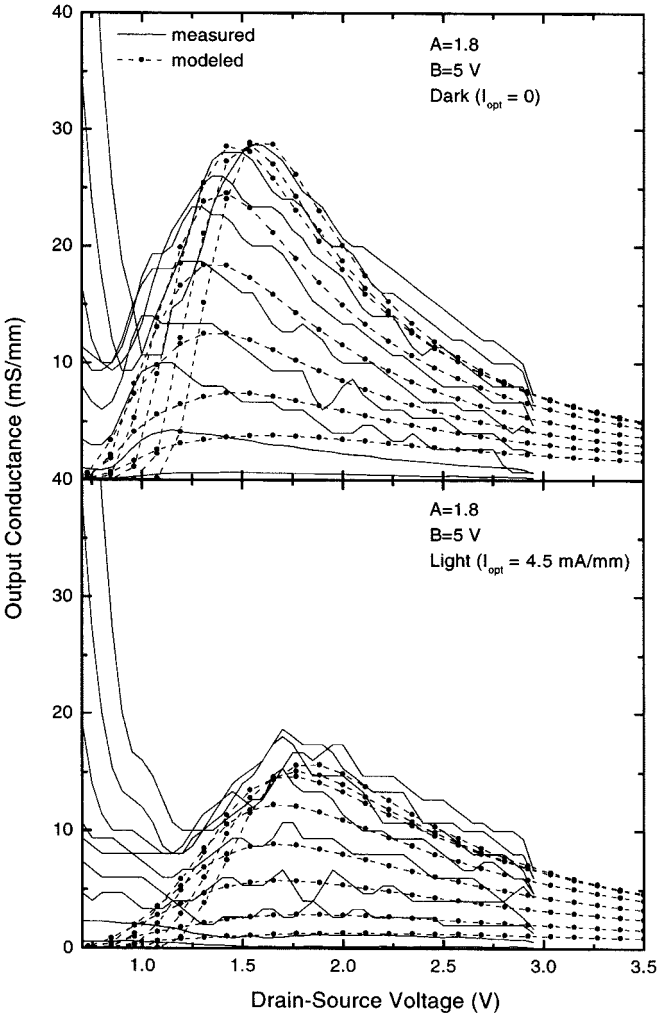

Fig. 12. Measured and modeled output conductance with and without illumination. Under illumination, the model explains the output conductance using the same fitting parameters with the addition of a bias-independent hole generation term. $T = 220$ K.

Given these results, it should be possible to model the kink both with and without illumination simply by adding a bias-independent current generator to our equivalent circuit model (see Fig. 1), where the value of the current is proportional to the optical generation rate. Fig. 12 plots the measured and modeled output conductance for both dark and relatively high-intensity illumination. Impressively, the addition of such a circuit element allows us to model both the light and dark kink output conductance *using identical impact ionization parameters*; the only parameter that is changed is the bias-independent optical generation rate.

E. Short Gate Lengths

Although our model appears to work well at the long gate lengths considered here, it is important to address the issue of

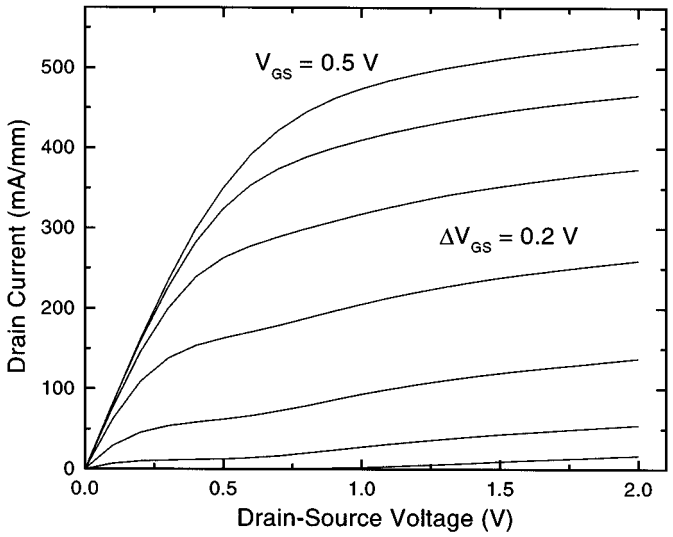

Fig. 13. Output characteristics for InAlAs/InGaAs double heterostructure HEMT with short gate length ($L_G = 0.2$ μm). Note the apparent disappearance of the kink at high V_{GS} values.

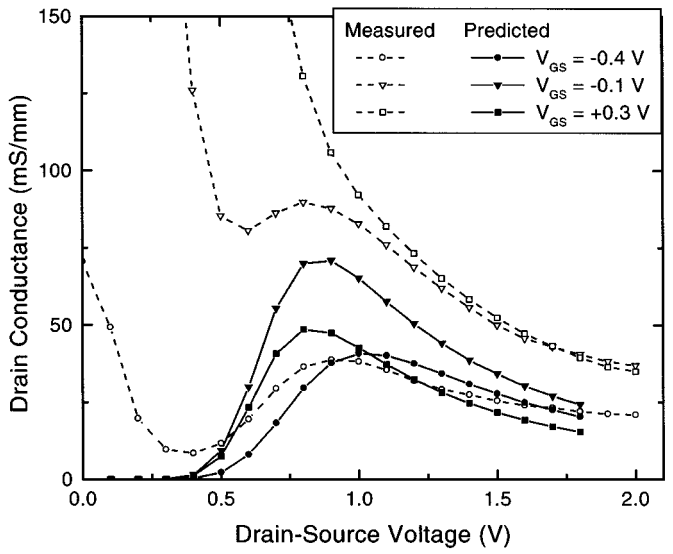

Fig. 14. Comparison of model predictions for output conductance with measured output conductance for device shown in Fig. 13.

portability to state-of-the-art, deep submicron gate length devices. Indeed, at shorter gate lengths, the kink appears more complicated. Fig. 13 plots a typical output characteristic for a state-of-the-art industrial HEMT with $L_G = 0.2$ μm. As can be seen, the kink is present at lower drain current, but seems to disappear as V_{GS} becomes more positive. Such behavior is found in many reported devices, and at first glance may seem inconsistent with the model presented here. However, comparison of the measured output conductance and the predicted kink output conductance (Fig. 14) for this device demonstrates that the kink may, in fact, be a major source of output conductance throughout the device's range of operation. The model accurately predicts the location and magnitude of the peaks in g_d for lower V_{GS} values; as V_{GS} increases, the model continues to predict the qualitative behavior of the kink well, but appears to underestimate the total output conductance by a constant. This is not surprising, as one would expect short channel effects to play a significant role in this device. Finally, at positive V_{GS} values, the peak in g_d is apparently obscured by the transition from the linear region to the saturation region, but the behavior of g_d still appears consistent with a *combination* of the kink effect and short channel effects. This suggests that in state-of-the-art devices, the kink may in fact be a major source of output conductance even at positive V_{GS} values, but is not visible on the output characteristics because of the soft transition from the linear region to the saturation region.

V. Summary and Conclusions

We have presented a new model for the kink effect in InAlAs/InGaAs HEMTS. Our model suggests that the kink arises from a process in which impact ionization generated holes travel from the drain-gate region through the intrinsic device and pile up in the extrinsic source. This hole pileup leads to a hole current to the surface and/or the buffer-substrate interface, which in turn changes the charge in these locations. As a result, the channel potential and electron concentration are raised, resulting in a shift in threshold voltage and extra gate drive to the transistor.

Our model leads to a simple equivalent circuit model description of the kink effect in these devices and in state-of-the-art deep submicron HEMT's. The model includes transient effects, uses only three bias-independent parameters, and works well for a wide range of biases and time scales. The model also helps explain the kink's structural, illumination, and temperature dependencies.

Acknowledgment

The authors wish to thank T. Suemitsu, T. Enoki, Y. Ishii, and N. Shigekawa of NTT Corporation for useful discussions, and B. Hoke of Raytheon for material growth.

References

[1] B. Georgescu, M. Py, A. Souifi, G. Post, and G. Guillot, "New aspects and mechanism of kink effect in InAlAs/InGaAs/InP inverted HFETs," *IEEE Electron Device Lett.*, vol. 19, pp. 154–165, May 1998.

[2] Y. Takanashi, K. Takahata, and Y. Muramoto, "Characteristics of InAlAs/InGaAs HEMT's under 1.3 μm laser illumination," *IEEE Electron Device Lett.*, vol. 19, pp. 472–474, Dec. 1998.

[3] T. Suemitsu *et al.*, "Mechanism and structural dependence of kink phenomena in InAlAs/InGaAs HEMTs," in *1997 Int. Conf. InP and Related Materials*, 1997, pp. 365–368.

[4] T. Suemitsu *et al.*, "An analysis of the kink phenomena in InAlAs/InGaAs HEMT's using two-dimensional device simulation," *IEEE Trans. Electron Devices*, vol. 45, pp. 2390–2399, Dec. 1998.

[5] G. Meneghesso *et al.*, "Improvement of DC, low frequency and reliability properties of InAlAs/InGaAs Inp-based HEMT's by means of an InP etch stop layer," in *IEDM Tech. Dig.*, 1998, pp. 227–230.

[6] J. del Alamo and M. Somerville, "Breakdown in millimeter-wave power InP HEMTs: A comparison with GaAs PHEMTs," *IEEE J. Solid State Circuits*, vol. 34, pp. 1204–1211, 1999.

[7] A. S. Brown *et al.*, "AlInAs-GaInAs HEMT's utilizing low-temperature AlInAs buffers grown by MBE," *IEEE Electron Device Lett.*, vol. 10, pp. 565–568, Dec. 1989.

[8] L. F. Luo, K. F. Longenbach, and W. I. Wang, "Kink-free AlInAs/GaInAs/InP HEMT's grown by molecular beam epitaxy," *Electron. Lett.*, vol. 26, no. 12, pp. 779–780, 1993.

[9] W. Kruppa and J. B. Boos, "Examination of the kink effect in InAlAs/InGaAs/InP HEMT's using sinusoidal and transient excitation," *IEEE Trans. Electron Devices*, vol. 42, no. 10, pp. 1717–1723, 1995.

[10] L. Aina and M. Burgess *et al.*, "0.33 μm gate length mm-wave InP channel HEMT's with high f_T and $f_{\max}$," *IEEE Electron Dev. Lett.*, vol. 12, pp. 483–485, Sept. 1991.
[11] D. R. Greenberg, J. A. del Alamo, and R. Bhat, "Impact ionization and transport in the InAlAs/n+InP HFET," *IEEE Trans. Electron Devices*, vol. 42, pp. 1574–1582, Sept. 1995.
[12] G. G. Zhou, A. F. Fischer-Colbrie, and J. S. Harris, "I-V kink in InAlAs/InGaAs MODFET's due to weak impact ionization in the InGaAs channel," in *6th Int. Conf. InP and Related Materials*, Mar. 1994, pp. 435–438.
[13] K. Kato, T. Wada, and K. Taniguchi, "Analysis of kink characteristics in SOI MOSFET's using two carrier modeling," *IEEE Trans. Electron Devices*, vol. ED-32, pp. 458–462, 1985.
[14] T. Suemitsu, T. Enoki, and Y. Ishii, "Body contacts in In*p*-based InAlAs/InGaAs HEMT's and their effects on breakdown voltage and kink suppression," *Electron. Lett.*, vol. 31, pp. 758–759, 1995.
[15] T. Zimmer *et al.*, "Kink effect in HEMT structures: A tra*p*-related semi-quantitative model and an empirical approach for spice simulation," *Solid-State Electron.*, vol. 35, pp. 1543–1548, Oct. 1992.
[16] M. H. Somerville, J. A. del Alamo, and W. Hoke, "A new physical model for the kink effect on InAlAs/InGaAs HEMTs," in *IEDM Tech. Dig.*, 1995, pp. 201–204.
[17] ——, "Direct correlation between impact ionization and the kink effect in InAlAs/InGaAs HEMTs," *IEEE Electron Device Lett.*, vol. 17, pp. 473–475, 1996.
[18] A. Ernst, M. Somerville, and J. A. del Alamo, "Dynamics of the kink effect in InAlAs/InGaAs HEMTs," *IEEE Electron Dev. Lett.*, vol. 18, pp. 577–579, Dec. 1997.
[19] Y. Hori and M. Kuzuhara, "Improved model for kink effect in AlGaAs/InGaAs heterojunction FETs," *IEEE Trans. Electron Devices*, vol. 41, pp. 2262–2266, Dec. 1994.
[20] M. Chertouk *et al.*, "Metamorphic InAlAs/InGaAs HEMT's on GaAs substrates with composite channels and $f_{\max}$ of 350 GHz," in *7th Int. Conf. InP and Related Materials*, 1995, pp. 737–740.
[21] C. Heedt *et al.*, "Drastic reduction of gate leakage in InAlAs/InGaAs HEMT's using a pseudomorphic InAlAs hole barrier layer," *IEEE Trans. Electron Devices*, vol. 41, pp. 1685–1689, Oct. 1994.
[22] T. Enoki, T. Kobayashi, and Y. Ishii, "Device technologies for In*p*-based HEMT's and their applications to ICs," in *IEEE GaAs IC Symp.*, 1994, pp. 337–339.
[23] K. Kunihiro, H. Yano, N. Goto, and Y. Ohno, "Numerical analysis of kink effect in HJFET with a heterobuffer layer," *IEEE Trans. Electron Devices*, vol. 40, pp. 493–497, Mar. 1993.
[24] B. Brar and H. Kroemer, "Influence of impact ionization on the drain conductance of InAs/AlSb quantum well HFETs," *IEEE Electron Dev. Lett.*, vol. 16, pp. 548–550, Dec. 1995.
[25] K. Hur, private communication, 1995.
[26] S. Bahl, private communication, 1997.
[27] N. Shigekawa, T. Enoki, T. Furuta, and H. Ito, "Electroluminescence of InAlAs/InGaAs HEMT's lattice-matched to InP substrates," *IEEE Electron Device Lett.*, vol. 16, pp. 515–517, Nov. 1995.
[28] D. Delagebeaudeuf and N. T. Linh, "Metal-(n)AlGaAs-GaAs two-dimensional electron gas FET," *IEEE Trans. Electron Devices*, vol. ED-29, pp. 955–960, June 1982.
[29] J. P. Colinge, *SOI Technology: Materials to VLSI*. Norwell, MA: Kluwer, 1991.
[30] A. A. Moolji, S. R. Bahl, and J. A. del Alamo, "Impact ionization in InAlAs/InGaAs HFETs," *IEEE Electron Device Lett.*, vol. 15, pp. 313–315, Aug. 1994.
[31] J. B. Kuang *et al.*, "Kink effect in submicrometer-gate MBE-grown InAlAs/InGaAs heterojunction MESFETs," *IEEE Electron Device Lett.*, vol. 9, pp. 630–632, Dec. 1988.
[32] G. Meneghesso and A. Mion *et al.*, "Effects of channel quantization and temperature on off-state and on-state breakdown in composite channel and conventional channel In*p*-based HEMTs," in *IEDM Tech. Dig.*, 1996, pp. 43–46.

Mark H. Somerville received the B.S. degree in electrical engineering and the B.A. degree in liberal arts from the University of Texas at Austin in 1990, the B.A. in physics from Oxford University, U.K., in 1992, and the M.S. and Ph.D. degrees in electrical engineering from the Massachusetts Institute of Technology (MIT), Cambridge, in 1993 and 1998 respectively. His doctoral research focused on fabrication, modeling and characterization of InAlAs/InGaAs HEMT's for power applications.

In September 1998, he joined the Department of Physics and Astronomy, Vassar College, Poughkeepsie, NY, as an Assistant Professor, where he is working to develop a system for spatially-resolved NIR emission spectroscopy. From 1989 to 1990, he was a systems engineer at SEMATECH, Austin, TX, where he worked on the development of modular automation approaches for semiconductor manufacturing. During this time, he also worked at the University of Texas on Monte Carlo simulation of InAlAs/InGaAs HBTs. At MIT, he conducted research on charge control and transport heavily-doped quantum wells from 1992 to 1993.

Alexander Ernst was born in 1971. He received the B.S. and M.S. degrees from the Massachusetts Institute of Technology (MIT), Cambridge, in 1997, and the M.B.A. degree in 1998 from the College des Ingenieurs, Paris, France.

Since then, he is a Consultant with McKinsey & Company, Mexico City, Mexico. He developed a new gate impedance measurement technique for characterizing mobility and sheet carrier concentration in HEMT's, and performed extensive work on the kink effect while at MIT.

Jesús A. del Alamo (SM'99) received the degree of Telecommunications Engineer from the Polytechnic University of Madrid, Spain, in 1980, and the M.S. and Ph.D. degrees in electrical engineering from Stanford University, Stanford, CA, in 1983 and 1985, respectively. He carried out his Ph.D. dissertation on minority carier transport in heavily doped silicon.

From 1977 to 1981, he was with the Institute of Solar Energy of the Polytechnic University of Madrid, working on silicon solar cells. From 1985 to 1988, he was a Research Engineer with NTT LSI Laboratories, Atsugi, Japan, where he conducted research on III-V heterostructure field-effect transistors. Since 1988, he has been with the Department of Electrical Engineering and Computer Science, Masschusetts Institute of Technology (MIT), Cambridge, where he is currently a Professor. His research insterests are on Gigahertz power transistors: Si LDMOS on SOI, GaAs PHEMT's and InP HEMT's.

Dr. del Alamo was an NSF Presidential Young Investigator from 1991 to 1996. In 1992, he was awarded the Baker Memorial Award for Excellence in Undergraduate Teaching at MIT. In 1993, he received the H. E. Edgerton Junior Faculty Achievement Award at MIT.